Zeitschrift: Schweizerische mineralogische und petrographische Mitteilungen = Bulletin suisse de minéralogie et pétrographie

Band: 72 (1992)

Heft: 1

Artikel: The volcanic activity in Syria and Lebanon between Jurassic and Actual

Autor: Mouty, M. / Delaloye, M. / Fontignie, D.

DOI: https://doi.org/10.5169/seals-54898

SCHWEIZ. MINERAL. PETROGR. MITT. 72, 91–105, 1992

The volcanic activity in Syria and Lebanon between Jurassic and Actual

by *M. Mouty* [1], *M. Delaloye* [2], *D. Fontignie* [2], *O. Piskin* [2] and *J.-J. Wagner* [2]

Abstract

Chemical compositions of lavas from the Dead Sea Rift System volcanism indicate a typical intraplate setting during the period between Jurassic and Actual. Whole rock Potassium-Argon geochronology on 43 basalts reveals a strong and general activity between Berriasian and Valanginian times and also a constant activity during the Tertiary but with a large gap between 16 and 8 Ma. The volume and timing of the volcanism is controlled by the left-lateral mouvement along the Rift.

Keywords: Geochronology, geochemistry, Dead Sea Rift, Syria, Lebanon.

1. Introduction

According to the scope of the present study, Western Syria can be divided both geographically and geologically in 5 major areas (Fig. 1):

a) The Coastal Range (Djebel Ansaryé) is situated in the North-western part of Syria. It is limited in the north by the river Nahr Al Kabir Al Shamali and in the south by the river Nahr Al Kabir Al Janoubi, by the depression of Ghab and Boukea (Rift Valley) in the east and by the Mediterranean Sea in the west. It is a N–S anticline cut by the Dead Sea Rift System on its Eastern flank (DUBERTRET, 1937).

b) The Aleppo Plateau is situated in the Northern part of Syria. Its limits are the Palmyride Range in the south, the river Euphrate in the east, the Kurd Dag in the north and the Mount Az-Zawyeh and the Ghab in the west. It is a large surface of horizontal Neogene sediments covered by extended lava flows.

c) The Palmyride Range is oriented NE–SW. It is the main structure of Central Syria and is in contact in the SW with the Anti-Lebanon chain and can be followed over 350 km to reach the river Euphrate. It is formed of many parallel anticlines. The central part is occupied by the Neogene bassin of Ad-Daw dividing this range in Southern and Northern Palmyrides.

d) The Lebanon and Anti-Lebanon ranges are situated between the Mediterranean Sea and the Palmyrides. Their direction is NNE–SSW. They represent two large monocline horsts separated by the Beeka graben (VAUTRIN, 1934; DUBERTRET, 1940). Large faults related to the Dead Sea Rift System cut anticlines and synclines.

e) The SW Plateau is limited in the west by the Jourdain valley, in the north by the Palmyrides, in the east by the dry plain of Badyet Al-Hamad. This plateau is mainly basaltic. It is a very large depression filled by volcanic flows. The parallel alignment of volcanoes oriented NW–SE is a remarquable feature. The center part of the plateau is occupied by the Djebel Al-Arab.

[1] Atomic Energy Commission and University of Damascus, Damascus, Syria.
[2] Department of Mineralogy, University of Geneva, 13, rue des Maraîchers, CH-1211 Geneva, Switzerland.

2. The volcanism of Syria

The Eastern Mediterranean (Lebanon and Syria) has undergone several volcanic phases from Jurassic to prehistorical time:

1. A first volcanic phase strictly located in the hart of the Mount Hermon anticline (Anti-Lebanon Range) started at the base of the Middle Jurassic (DUBERTRET, 1933). It is represented by a 50 m thick layer in a shallow water dolomitic limestone (Fig. 2). Field observations do not allow to decide between a flow or a sill. Dubertret and Vautrin attributed a Bajocian age to this volcanism because of its stratigraphic position below palaeontologically dated Bathonian limestones.

2. A second phase appears in the Mount Lebanon during the Upper Jurassic (Oxfordian). An ash layer with a very limited extension is interbedded in a predominantly marly limestone but also oolithic sparitic limestone rich in corrals and stromatopores. This facies bear witnesses for a shallow medium and was named by Dubertret "Niveau de Bhannes".

3. The volcanic activity increased at the end of the Jurassic (Portlandian) in the Northern part of Lebanon and in Southern Anti-Lebanon (Mount Hermon). Basaltic flows are interlayered in bioclastic limestone levels deposited in very shallow high energy sea-environment. At that time, most of the Arabian peninsula was emerged except a few areas like the NW platform; the volcanism started just before the emergence of the latter.

4. A new volcanic phase took place in the western and north-western areas (e.g. Bloudane and Wadi Al Karn in the Anti-Lebanon) just before the large Cretaceous marine transgression occurring during Neocomian and Aptian stages (Fig. 3). The volcanism reached also the central part of the Palmyrides and can be seen in the Jebel Rmah and in a well near Al Karyatein. In the north (Coastal Range) this phase has been eroded nevertheless it can be observed as remnants in palaeokarsts (Joubet Barghal, Joubet Rband). Although highly weathered, it contains well preserved deep crustal xenoliths such as granitoids, amphibolites and granulites.

5. The next volcanic phase started in Upper Albian to Cenomanian in the north of Lebanon and in the central part of the Syrian Coastal Range (Fig. 4). In this later region, the lava flow is an augite bearing basalt interbedded in a neritic limestone with an Upper Albian microfauna (MOUTY and SAINT-MARC, 1982). This flow lays on ripple marks indicating the shallow depth of the sea; no baked contact has been observed. The sedimentary cover of the flow shows an uneven base with basaltic elements. This flow probably

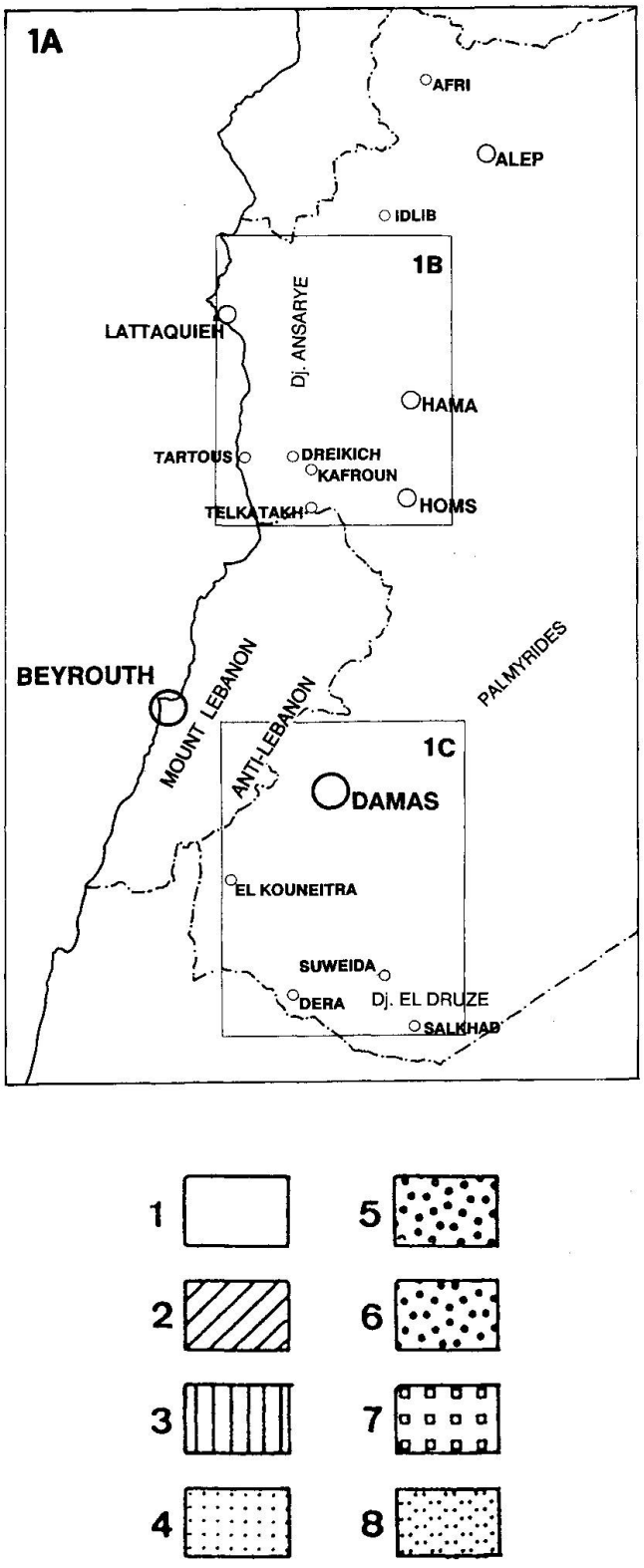

Fig. 1 A) Geographical and geological situation of studied areas. 1 = Quaternary sediments; 2 = Pliocene sediments; 3 = Jurassic and Cretaceous sediments; 4 = Upper Miocene volcanics; 5 = Pliocene volcanics; 6 = Early Quaternary volcanics; 7 = Middle Quaternary volcanics; 8 = Recent volcanics.

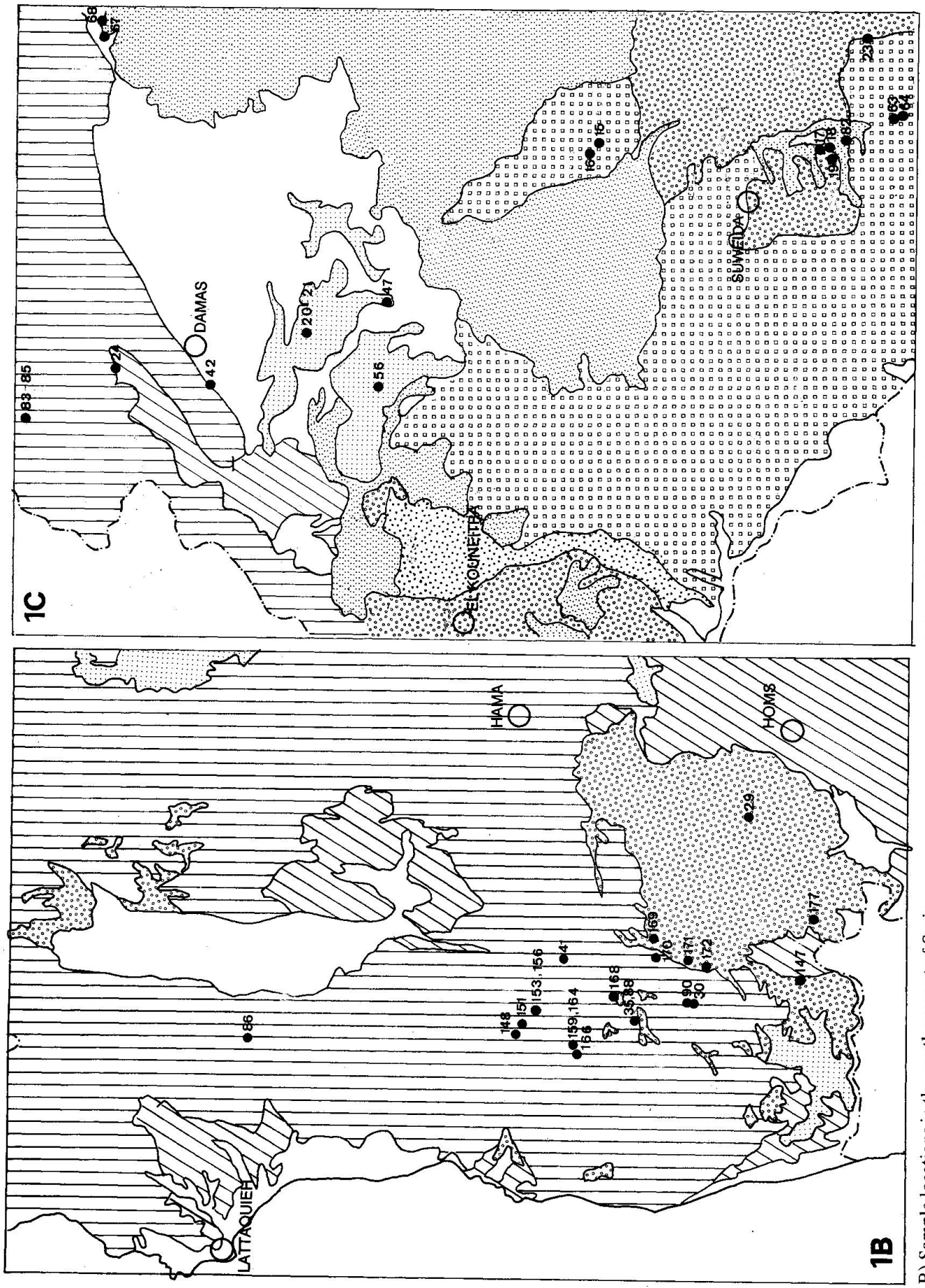

C) Sample locations in the southern part of Syria.

B) Sample locations in the northern part of Syria.

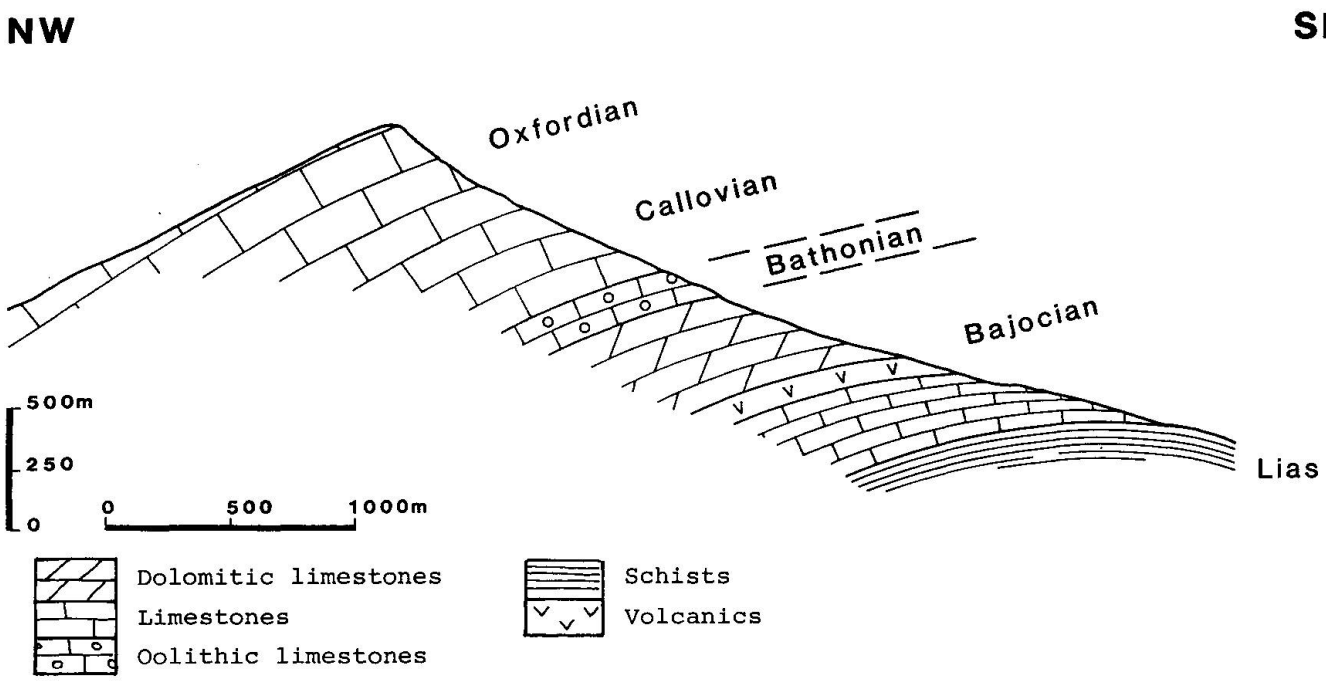

Fig. 2 Geological cross-section of Mount Hermon (Anti-Lebanon Range). Basalts underlie Bajocian limestones.

originating near Wady Al Ouyoun has a maximum thickness of 50 meters. Eastwards, it thins out, gradually replaced by volcano-detritic layers and finally desappears. Its extension is of 50 km^2 between Qadmous in the north and Marmarita in the south.

6. The Palaeogene volcanism can be observed near the Aafrine Valley (NW from Aleppo) as

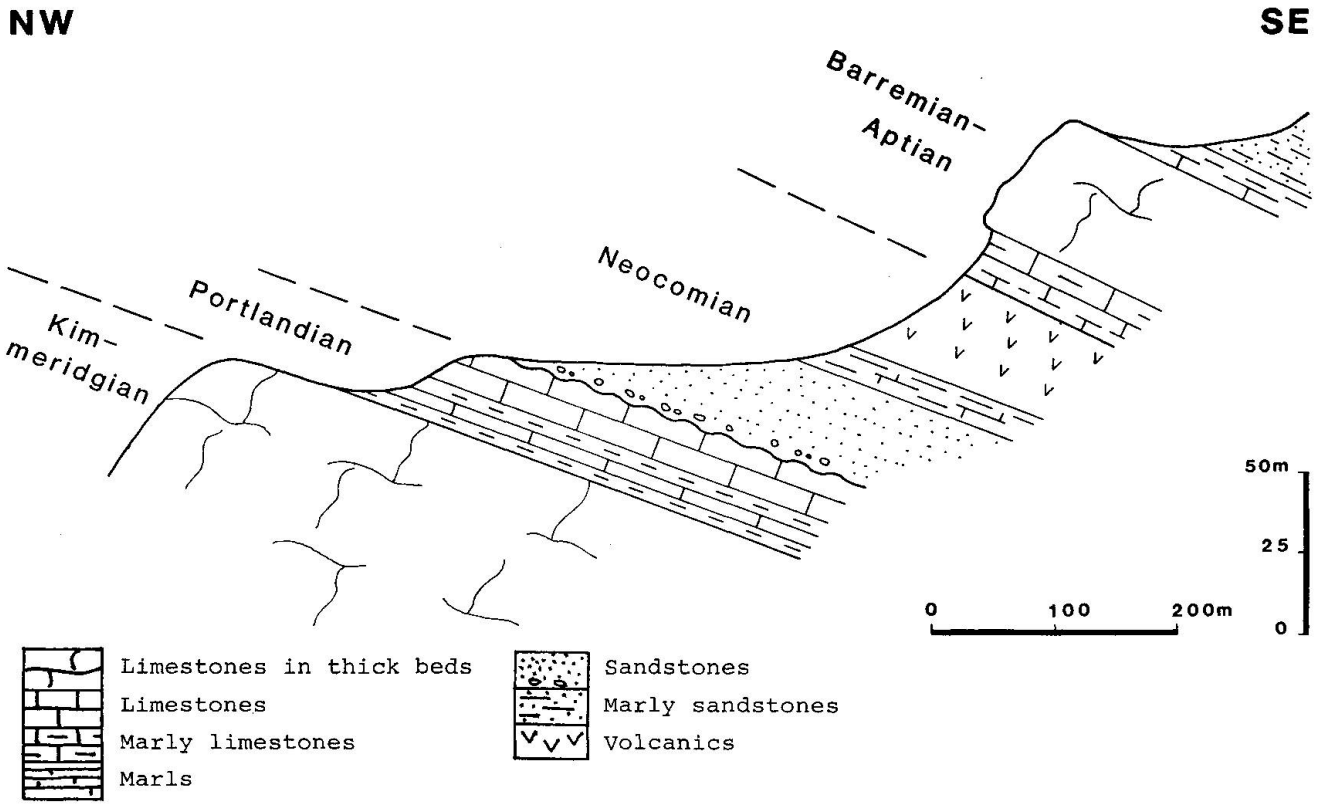

Fig. 3 Geological cross-section near Bloudane (Coastal Range) presenting the basalts interbedded in Necommian limestones.

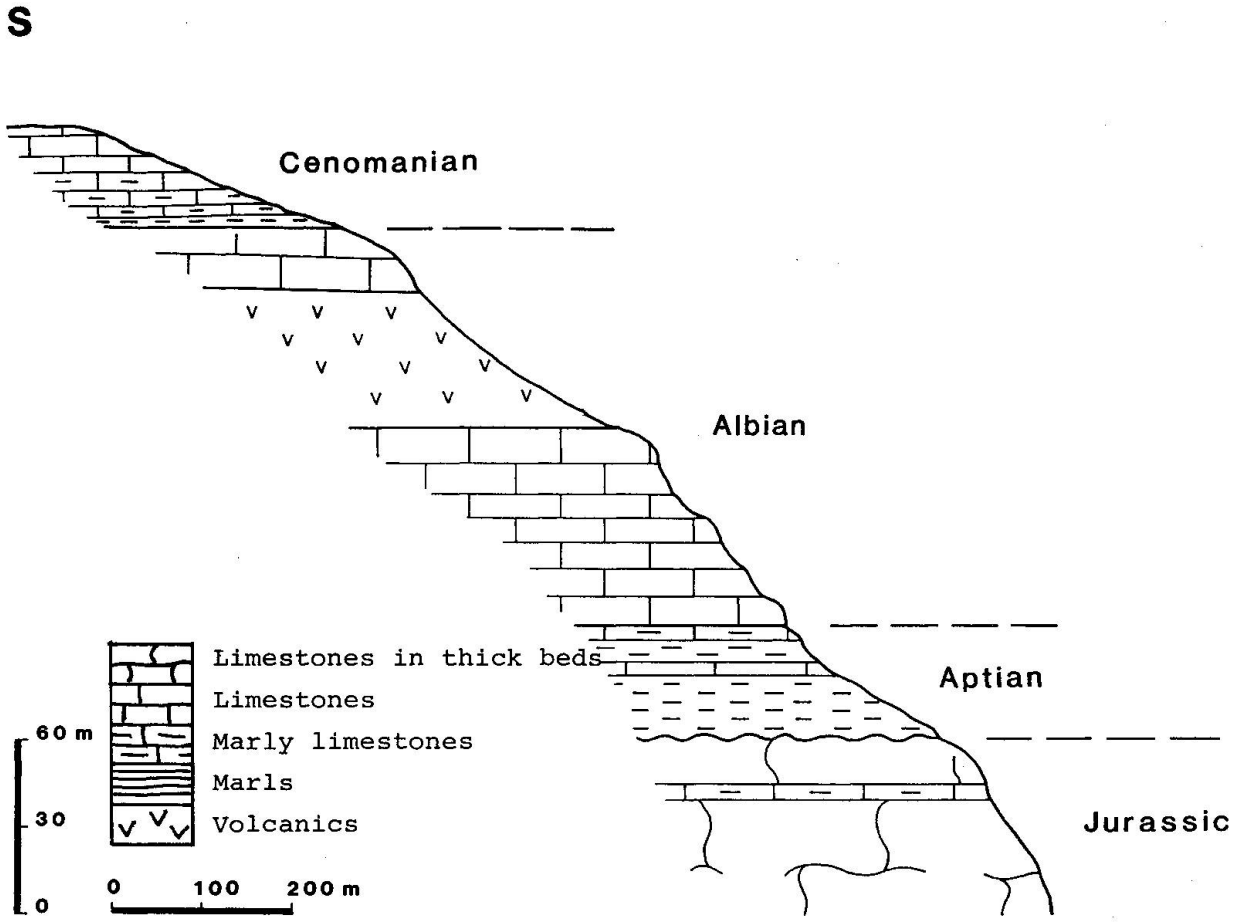

Fig. 4 Geological cross-section near Wadi Al Ouyoun (Coastal Range) showing the thick basaltic flow interbedded in the Albian sediments as seen on the western flank of the rift (Al Ghab).

tuffs and also some altered basaltic blocks in the upper part of the Lower Eocene. These marly limestone bearing pelagic fauna indicate a deep sedimentation. These volcanic products do not appear elsewere in the area.

7. In the Lower Miocene, when the Arabian plateform is almost completely emerged, a very strong volcanic activity begins. It covers sedimentary layers of Oligocene, Upper Eocene, post-Palaeogene continental deposits in the Palmyride and Damascus area. Near Aleppo, lava flows are interbedded in Helvetian marine sediments of Middle Miocene.

8. After a relatively quiet period, the volcanism is again active in Pliocene times. In the Coastal Range, the Pliocene dated flows cover an eroded surface cutting the Jurassic in the east and the Pliocene in the west. Finally, near Tartous the flows are interbedded in the Pliocene formations. Volcano-detritic formations related to these flows are observed in depressed areas near Bannias. Remnants can be observed on top of many hills (from E to W: Btar, Mechta, Kafroun, Chaara, Marmarita and Maten) where typical columnar jointing is visible (Fig. 5).

9. Quaternary volcanism developped in SW Syria over large areas (Hauran, Djebel Al Arab). The last eruption occurred in historical times.

3. Geochronology

The age span (Jurassic to Actual) and the type of rocks normally associated to the intra-plate volcanism (basalts and tholeiites) limit the choice of the analytical method to the Potassium-Argon and the choice of the samples to whole rock only (location of samples table 1).

43 age measurements have been performed in our dating laboratory. Analytical data are summarized in table 2.

3.1. ANALYTICAL METHOD

Chemical analysis of Potassium and isotopic analysis of Argon are made on aliquotes of crushed rock samples whose granulometry is between 100 and 250 mesh. Potassium is measured twice on two rock fractions using Atomic Absorp-

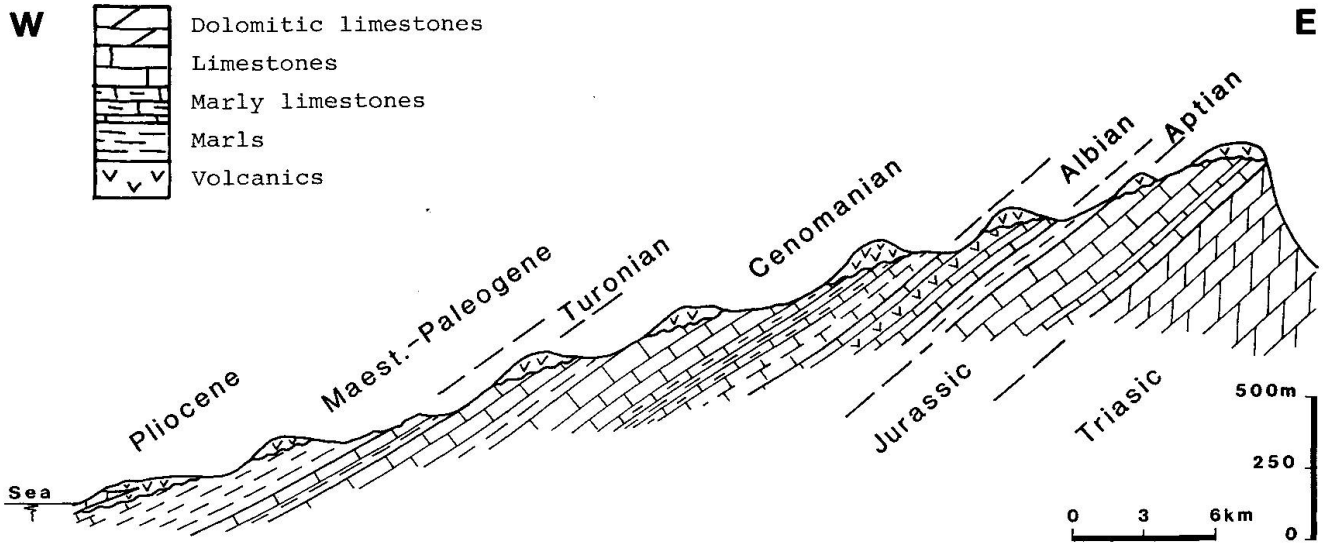

Fig. 5 Geological cross-section near Machta in the Coastal Range showing the deposition of basaltic flows on an erroded and tilted post-Maestrichtian surface.

tion (Pye-Unicam 9000). The values reported in table 2 correspond to the mean of the two measurements. Isotopic analysis of Argon is made using isotopic dilution on an AEI-MS-10-S mass spectrometer equiped with computer acquisition of the data (DELALOYE and WAGNER, 1974; FONTIGNIE, 1980). Constants used are those recommended by STEIGER and JÄGER (1977). LP-6 and HD-B1 international standards are used for calibration.

3.2. JURASSIC

Six samples have been collected from flows interbedded in sediments or in karst-fillings. Most of these give rejuvenated ages due principally to the alteration of the rock. This is the case in Rimeh, Arneh and Qalaat Jandal with lavas intercalated at the base of Middle Jurassic and showing apparent ages close to 120 Ma instead of the expected 170 Ma according to the geological setting. They are not reported in the tables.

3.3. CRETACEOUS

Outcrops of Cretaceous volcanism are observed in the Coastal Range, in the Anti-Lebanon Range and in the Palmyride Range. They show Albian ages ranging between 93 and 114 Ma. The sample from Joubet Barghal gives an age of 109 Ma (Aptian) also compatible with the palaeontological determination.

In the Anti-Lebanon Range, near the village of Bloudane, basalts occur just below palaeontologically dated Barremian marly limestones (126–130 Ma). Four dates indicate a Valanginian age between 119 and 127 Ma.

3.4. MIO-PLIOCENE

32 age determinations have been made on Neogene volcanics collected in the Coastal Range, on the Aleppo Plateau, in the Palmyrides, in the Anti-Lebanon Range and on the SW Syrian Plateau. This volcanism started 24 Ma ago at the base of the Miocene and finishes around 16 Ma in Middle Miocene. This first phase is present in all regions except in the Coastal Range. A large gap in the activity exist between 16 and 8.5 Ma (Fig. 6). At that time eruptions begin again in all regions except in the Anti-Lebanon. The opening of the Rift, particularly in the Ghab and Boukea areas, is well documented by lava flows dated both radiometrically and palaeontologically. Our measurements are of confidence up to 1.5 Ma but the volcanic activity lasted almost to historical times as it is demonstrated in the northernmost part of the Rift, in the Karasu Valley (CAPAN et al., 1987) where ages range from about 2 Ma to 0.4 Ma.

3.5. CONCLUSIONS

Though Jurassic volcanism is present in Syria, alteration of the rocks do not allow precise K–Ar age determinations. During Cretaceous times, basalts are dated from Berriasian and Valanginian, synchronous with the opening of the south Atlantic Ocean.

Tab. 1 List of analysed samples with geographic location and geodesic coordinates.

Sample Nb	Locality	Coordinates (Longitude/Latitude)
S 15	Tell Thannoun	36°43/32°56
S 16	Tell Thannoun	36°43/32°56
S 17	Sud de Al Kafr	36°39/32°37
S 18	Al Kafr	36°39/32°37
S 19	Al Kafr	36°39/32°37
S 20	Djebel Abu Nagib	36°19/33°21
S 21	Djebel Abu Nagib	36°19/33°21
S 23	Howeha	36°52/32°33
S 24	Halboun	36°15/33°38
S 29	Route Homs - Tartous - Shin	36°37/34°47
S 30	Machta près de Kafroun	36°17/34°47
S 31	Kafroun	36°12/34°50
S 35	Zaghrine	36°12/34°56
S 41	Massiaf	36°18/35°03
S 43	Route Alep - Blas	37°11/36°06
S 44	Blas	37°11/36°04
S 45	Blas	37°11/36°04
S 47	El Ajam	36°22/33°14
S 56	Tell Abou Aba	36°14/33°29
S 63	Salkhad	36°42/32°23
S 64	Salkhad	36°42/32°23
S 67	Abou Ash-Shamat	36°52/33°38
S 68	Abou Ash-Shamat	36°52/33°38
S 71	Nord de Rmah	37°28/34°07
S 72	Sud de Rmah	37°30/34°13
S 82	Tall Al Amar	36°43/33°37
S 83	Bloudane (Abu Zad)	36°10/33°45
S 84	Bloudane (Abu Zad)	36°10/33°45
S 85	Bloudane (Abu Zad)	36°10/33°45
S 86	Joubet Barghal	36°09/35°29
S 88	Avant Zaghrine	36°12/34°56
S 90	Djebel Mechta	36°17/34°47
S141	Rmah	37°30/34°04
S147	Mallouaa	36°12/34°50
S148	Djebel Molla Hassan	36°10/35°06
S151	Djebel Zaghrine	36°10/35°05
S154	Djebel Zaghrine	36°13/35°07
S155	Djebel Zaghrine	36°13/35°07
S159	Beit Hadjou	36°10/35°01
S162	Brommanet Al-Machayekh	36°10/35°01
S166	Brommanet Al-Machayekh	36°10/35°01
S170	Mesheyrfi	36°13/34°54
S177	Beka	36°23/34°46

The beginning of a new phase of activity at the base of the Miocene is contemporaneous with the beginning of the collision between the Arabian Plate and the Eurasian Continent and also with the opening of the Red Sea. It is also the time where the W–E mouvement of the Afro-Arabian block changes to an almost S–N mouvement.

Age determinations, tectonic and stratigraphic constraints discussed by CAMP and ROOBOL (1989) about continental alkali basalts of Western Saudi

Tab. 2 Potassium-Argon analytical data.

Sample number	% K	Age in Ma	$^{40}Ar^{*}$ x10^{-10} moles/g	$\%^{40}Ar^{*}$	$^{40}Ar/^{36}Ar$	$^{40}K/^{36}Ar$ x10^{3}
S 15	1.58	1.7 ± 0.1	0.48	19	365	68.71
S 16	1.52	1.5 ± 0.1	0.41	18	360	72.57
S 17	2.06	5.5 ± 0.2	1.98	53	632	104.29
S 18	1.73	4.6 ± 0.2	1.39	51	609	116.21
S 19	3.98	4.5 ± 0.1	3.09	77	1279	378.81
S 20	1.75	19.2 ± 0.6	5.85	80	1443	102.18
S 21	1.21	16.7 ± 0.6	3.49	56	677	39.05
S 23	1.56	2.8 ± 0.1	0.77	64	812	313.21
S 24	0.51	18.5 ± 0.4	1.65	12	337	3.86
S 29	0.68	5.5 ± 0.1	0.65	22	377	25.45
S 30	0.47	126.2 ± 2.7	10.61	50	588	3.85
S 31	1.03	8.1 ± 0.2	1.46	22	378	17.57
S 35	1.11	100.7 ± 2.2	19.87	65	848	9.18
S 41	1.07	125.0 ± 3.1	23.92	89	2652	31.34
S 43	0.51	18.0 ± 0.4	1.58	32	437	13.49
S 44	0.42	16.7 ± 0.5	1.23	25	394	10.09
S 45	0.42	17.5 ± 0.5	1.28	23	385	8.77
S 47	0.96	16.7 ± 0.5	2.79	16	351	5.67
S 56	0.56	24.0 ± 0.6	2.35	65	850	39.41
S 63	1.07	2.4 ± 0.1	0.45	14	345	35.28
S 64	0.64	2.5 ± 0.2	0.28	22	377	55.05
S 67	0.43	20.6 ± 0.5	1.53	44	524	19.01
S 68	0.53	19.3 ± 0.4	1.78	39	481	16.45
S 71	0.73	20.2 ± 0.4	2.56	51	601	25.92
S 72	1.08	8.3 ± 0.2	1.55	44	527	47.91
S 82	1.88	2.4 ± 0.1	0.78	18	361	47.16
S 83	1.19	124.0 ± 2.6	26.47	60	740	5.95
S 84	1.03	127.5 ± 2.9	23.56	80	1452	15.07
S 85	1.06	125.0 ± 2.7	23.74	48	570	3.65
S 86	3.44	108.9 ± 2.6	66.96	88	2566	34.81
S 88	1.33	93.2 ± 2.8	22.07	75	1204	16.34
S 90	1.11	14.6 ± 1.2	2.82	11	333	4.44
S 141	0.72	23.5 ± 0.7	2.97	29	414	8.65
S 147	1.51	8.5 ± 0.8	2.21	10	327	6.48
S 148	0.68	4.6 ± 0.1	0.54	38	475	67.57
S 151	1.11	12.4 ± 0.5	2.41	40	497	27.81
s 154	0.98	6.9 ± 0.2	1.17	29	416	30.23
S 155	1.41	6.8 ± 0.3	1.67	45	535	60.22
S 159	2.25	5.6 ± 0.5	2.21	24	391	29.01
S 162	0.72	92.6 ± 2.1	11.85	79	1401	20.02
S 166	0.69	93.2 ± 2.1	11.39	62	769	8.52
S 170	1.75	5.1 ± 0.1	1.55	16	352	19.01
S 177	0.81	5.4 ± 0.1	0.75	24	391	30.19

Arabia suggest that the first stage of spreading of the Red Sea took place 30 Ma ago and lasted 15 Ma. After a gap, the second stage of spreading started 5 Ma ago. This is in good concordance with our results on rocks from the Syrian segment of the Dead Sea Rift.

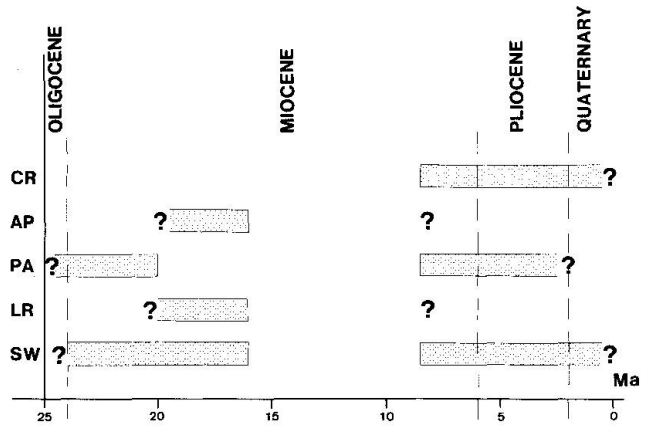

Fig. 6 Neogene K–Ar age distribution within the principal areas of Syria. CR = Coastal Range; AP = Aleppo Plateau; PA = Palmyride Range; LR = Lebanon and Anti Lebanon Range; SW = Southwestern Plateau.

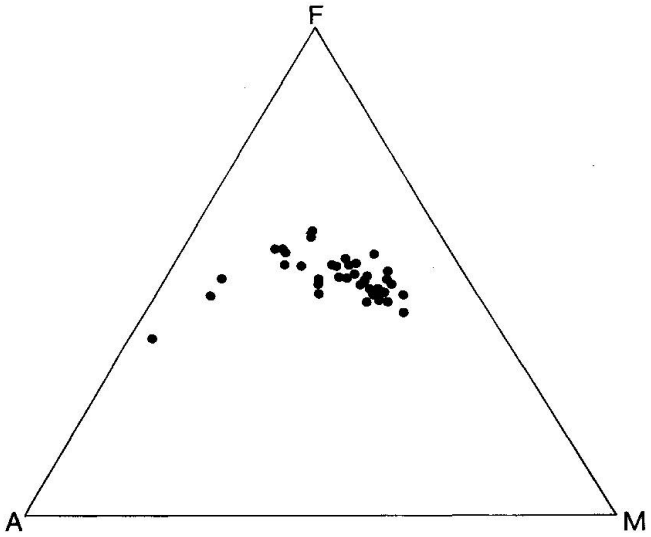

Fig. 7 AFM Diagram showing the differentiation trend of Syrian basalts.

4. Geochemistry

4.1. INTRODUCTION

In order to characterize the Syrian volcanism, major and trace elements are used in FMA, Alk–SiO_2,Ti–Zr, Ti–Zr–Y or Ni–MgO diagrams. Major element values are corrected according to IRVINE and BARAGAR (1971) recommendations.

4.2. ANALYTICAL PROCEDURES

Whole-rock chemical analyses were made at Geneva University using a Philips PW 1410 wavelength-dispersive XRF on $Li_2B_4O_7$ beads (20% rock, 80% flux by weight) prepared from rock powder, after loss on ignition. A ZAF matrix-effect correction was applied for major elements analysis and interelement corrections applied for traces. X rays were produced by an Ag anode tube. Counting times vary between 10 and 100 seconds depending on the element. USGS and CRPG (Nancy, France) standard rocks were used. H_2O content was measured using the Penfield gravimetric method on dry rock powders. FeO was measured using the Pratt colorimetric method with Dipyridyl reagent.

Trace elements are measured on pressed pellets of dry powdered rock mixed with 25% cellulose as a binding agent.

Both for major and trace elements, standards are prepared in the same way as unknown samples. Matrix effects and interelements overlapping are automatically corrected using a Philips-Zurich developed computer programm.

4.3. MAJOR- AND TRACE-ELEMENTS

(Data are collected in table 3.) Both AFM (Fig. 7) and $Na_2O + K_2O$ vs SiO_2 (Fig. 8) diagrams document the intermediate character of the Syrian lavas. It is worth to note that Quaternary and Cretaceous rocks are much more clustered, whatever the geographic situation, in comparison to the Neogene rocks. In general, all lavas are more on the alkaline and calco-alkaline side than in the tholeiitic side.

SiO_2 varies between 40 and 52%, Al_2O_3 between 11.5 and 17.8; TiO_2 between 0.9 and 3.3; $FeO + Fe_2O_3$ between 6.6 and 13.8%; $Na_2O + K_2O$ between 3 and 8% for the large majority of the samples. Only few of them are richer in SiO_2 and in alkalies like the benmoreites and trachytes. The chemical classification groups all rocks in the three fields of basalts, hawaïtes and tephrite-basanite (Fig. 8).

Ti vs Zr (Fig. 9), Ti–Zr–Y (Fig. 10) and Cr vs Y (Fig. 11) discrimination diagrams show that the analysed samples are well located in the "Within Plate Lava" fields. The Syrian Cretaceous to Actual volcanism though appears as typical of this type of environment.

The diagram Ni vs MgO (Fig. 12) after AUCHAPT et al., 1987 show straight lines of 5% and 25% where partial melting liquids are supposed to be represented. Curved lines of 5% and 10% represent fractional crystallization of olivine and/or cpx. It is worth noting that, here also, Cretaceous and Quaternary samples are much more clustered than Neogene samples. Moreover, Cretaceous and Quaternary samples never over-pass the 5% partial melting line. They are also grouped close

Tab. 3 Chemical analysis for major and trace elements.

No	SiO_2	Al_2O_3	TiO_2	FeO	Fe_2O_3	CaO	MgO	Na_2O	K_2O	MnO	P_2O_5	H_2O	CO_2	Sum	Ni	Cr	Zr	Y
S 15	44.27	14.19	2.75	7.80	4.24	8.84	9.92	3.45	1.96	0.18	0.72	1.00	0.00	99.32	317	412	320	25
S 16	44.40	15.52	2.94	7.41	4.44	9.66	7.03	3.45	1.83	0.25	0.79	0.97	0.35	99.04	106	204	288	26
S 17	49.67	16.89	2.70	7.64	4.21	6.72	3.39	4.02	2.44	0.18	0.85	0.94	0.33	99.98	5	46	455	34
S 18	49.33	16.96	2.46	7.86	3.96	6.58	3.91	4.03	2.21	0.24	0.79	0.77	0.33	99.43	19	101	352	30
S 19	59.45	17.83	0.86	4.16	2.36	1.75	0.72	5.93	4.80	0.15	0.16	0.75	0.00	98.92	2	39	846	32
S 20	45.90	16.88	2.72	8.42	4.22	7.43	4.61	4.57	2.77	0.14	0.71	1.00	0.03	99.40	55	120	346	22
S 21	47.19	14.49	2.80	7.89	4.33	9.34	7.13	2.86	1.47	0.18	0.69	1.02	0.00	99.39	263	350	227	24
S 23	49.49	16.61	2.94	7.05	4.45	8.12	3.61	4.07	1.92	0.18	0.59	0.52	0.10	99.65	3	54	300	35
S 24	47.88	15.21	1.79	8.54	3.40	10.16	7.38	2.39	0.68	0.15	0.29	1.07	0.38	99.32	225	338	133	19
S 29	44.64	15.32	3.13	8.05	4.66	9.22	7.50	3.42	0.97	0.27	0.65	1.00	0.26	99.09	160	266	255	26
S 30	47.68	14.17	2.03	8.31	3.52	8.87	9.32	2.80	0.69	0.16	0.27	1.00	0.00	98.82	231	322	129	21
S 31	40.60	12.43	3.05	8.49	4.15	12.21	10.89	3.69	1.34	0.29	1.17	1.00	0.00	99.31	223	326	263	29
S 35	43.75	13.29	2.56	8.75	3.07	11.76	9.96	2.68	1.48	0.25	0.59	1.01	0.00	99.15	213	362	160	25
S 41	44.23	14.18	2.75	7.61	4.26	8.83	9.90	3.43	1.96	0.18	0.72	1.00	0.00	99.05	180	275	246	25
S 43	51.19	14.01	1.54	6.98	3.16	8.86	8.11	2.96	0.68	0.15	0.23	1.08	0.38	99.33	282	301	101	22
S 44	51.85	13.96	1.58	7.26	3.09	9.10	8.02	3.44	0.58	0.15	0.24	1.00	0.36	100.63	291	329	117	23
S 45	52.97	14.28	1.56	6.93	3.07	8.80	6.96	2.98	0.54	0.15	0.27	1.00	0.37	99.88	269	275	111	24
S 47	48.62	16.24	2.23	6.88	3.73	10.00	5.56	3.42	1.09	0.17	0.45	0.70	0.08	99.17	79	125	176	25
S 56	47.37	14.78	2.10	8.18	3.60	9.06	9.59	2.65	0.81	0.18	0.36	0.55	0.13	99.36	240	324	164	22
S 63	47.49	16.83	2.61	7.78	2.88	10.32	5.79	3.18	1.31	0.17	0.50	0.40	0.36	99.62	36	31	204	28
S 64	48.24	16.01	2.10	7.51	3.60	10.12	7.85	3.27	0.86	0.18	0.34	0.13	0.11	100.32	92	255	161	27
S 67	47.15	14.26	1.54	8.99	3.05	9.51	11.32	2.80	0.67	0.18	0.28	0.55	0.37	100.67	352	368	99	19
S 68	46.64	14.22	1.66	9.75	3.16	9.86	9.67	2.78	0.65	0.20	0.23	0.95	0.36	100.13	324	360	107	17
S 71	47.72	14.27	2.21	7.00	3.80	10.11	7.68	3.26	1.02	0.17	0.40	0.86	0.37	98.87	210	319	141	18
S 72	45.07	15.98	2.88	7.55	4.41	10.73	6.42	2.94	1.35	0.18	0.20	1.02	0.37	99.10	113	190	195	24
S 82	44.70	15.13	3.03	9.62	4.17	7.23	5.90	5.14	2.21	0.19	0.98	0.83	0.11	99.24	68	129	407	22
S 83	47.52	14.94	3.25	8.20	4.85	8.42	4.65	3.68	1.47	0.26	1.38	1.01	0.00	99.63	8	18	299	46
S 84	47.48	14.80	3.26	8.19	4.78	8.60	4.48	3.47	1.35	0.25	1.37	1.01	0.36	99.40	6	12	296	46
S 85	47.50	14.87	3.18	8.25	4.71	8.55	4.46	3.47	1.36	0.24	1.35	1.01	0.36	99.31	12	20	299	45
S 86	55.54	16.52	0.65	6.97	2.17	4.39	1.97	5.18	4.18	0.17	0.61	1.01	0.36	99.72	1	12	673	34
S 88	46.16	13.69	2.20	9.30	2.62	9.23	10.23	3.33	1.32	0.18	0.46	1.00	0.00	99.72	222	532		
S 90	41.45	13.31	2.76	7.77	4.28	12.21	10.57	3.15	1.36	0.18	1.31	1.00	0.00	99.35	192	344	212	27
S141	48.83	14.41	2.34	7.87	3.96	7.67	7.54	3.51	1.06	0.17	0.42	1.08	0.39	99.25	270	328	154	23
S147	48.21	16.81	2.73	8.87	4.4	0.41	8.03	0.03	7.87	0.06	0.57	1.11	0.40	99.50	363	366	208	23
S148	43.12	12.07	2.51	8.88	4.07	7.70	13.62	3.54	1.02	0.19	1.27	1.01	0.37	99.37	369	412	235	24
S151	43.59	13.02	2.72	8.27	4.28	8.36	11.30	3.47	1.19	0.17	1.41	1.04	0.37	99.19	311	301	251	25
S154	45.66	15.09	3.37	10.38	3.47	4.30	8.76	4.23	1.73	0.19	1.32	0.83	0.39	99.72	108	131	278	27
S155	45.18	14.52	3.05	9.19	4.60	6.76	8.13	3.17	1.76	0.20	1.08	1.02	0.37	99.03	128	169	251	26
S159	47.25	15.54	2.61	8.57	3.93	5.73	6.79	4.19	2.49	0.17	1.04	1.05	0.36	99.72	137	207	314	24
S162	45.95	13.80	2.29	9.42	3.14	9.76	9.49	2.69	1.26	0.17	0.54	1.00	0.30	99.81	187	242		
S166	41.96	13.83	3.35	8.46	3.76	11.10	9.84	3.15	1.65	0.19	0.99	1.00	0.24	99.52	151	204	214	27
S170	46.40	15.25	3.08	8.49	3.67	7.77	6.79	4.51	2.22	0.16	0.67	1.00	0.00	100.01	102	142	293	22
S177	44.31	14.59	2.83	8.94	4.33	9.73	7.67	3.83	1.04	0.18	1.27	1.00	0.05	99.77	159	243	244	28

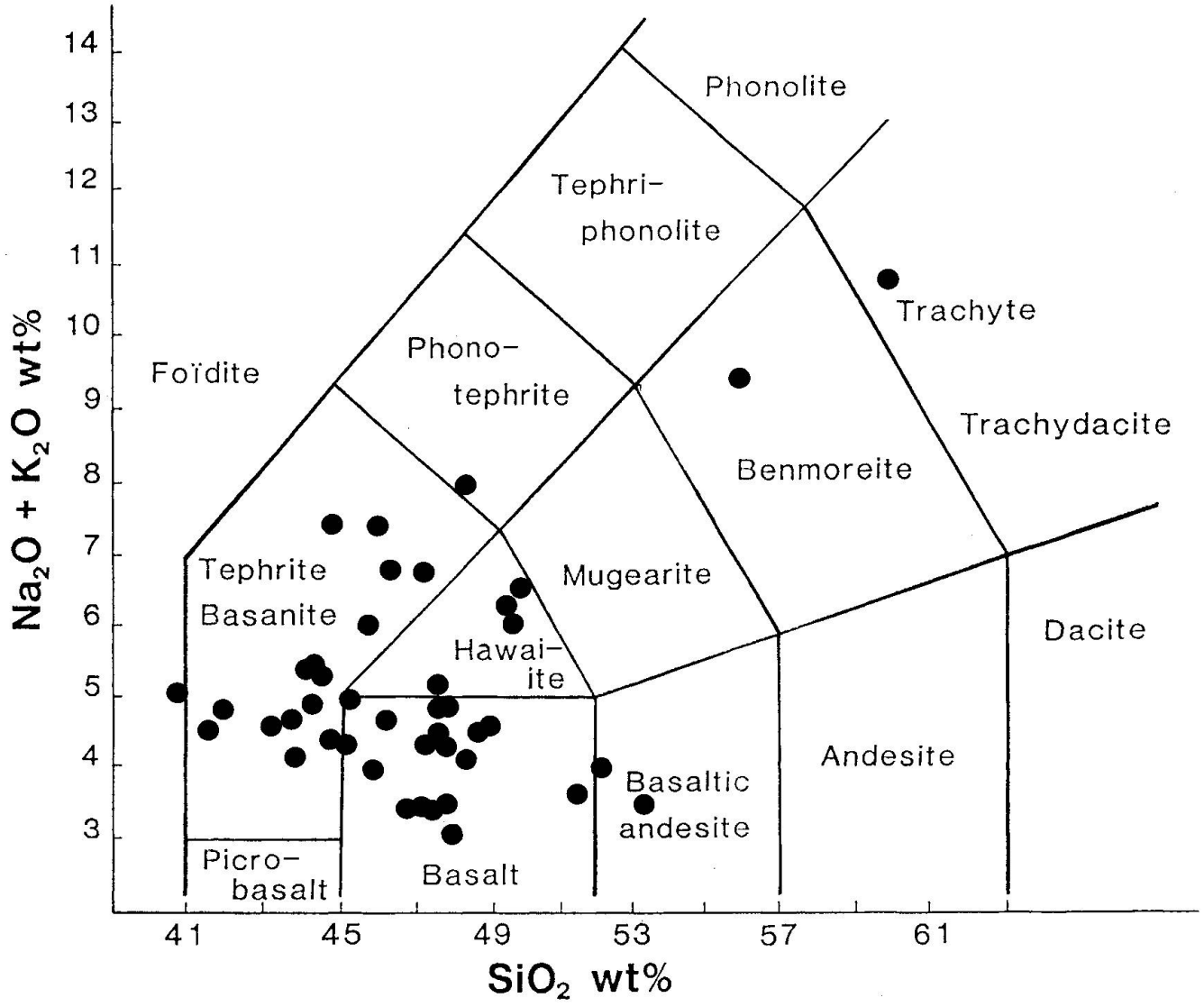

Fig. 8 Alkalis vs Silica diagram (LEBAS et al., 1983) is used to classify the analysed rocks. Their intermediate character is well demonstrated despite some particular composition explained in the text.

but below the 10% fractional crystallization line. This implies a larger partial melting during Neogene time perhaps due to a stronger volcanic activity or a stronger heat flow related to a greater mouvement of the Arabian plate.

Six whole rocks have been analysed for REE and show the typical pattern (Fig. 13) of alkali basalts in a continental crust environment ($K_2O + Na_2O = 5.1$; $K_2O/Na_2O = 0.48$) moderately enriched in LREE compared to HREE. The ration La/Lu_{CN} varies between 9.8 and 20.0 and could represent partial melting of spinel peridotite. A small negative Eu anomaly is present in all six samples.

5. Petrology

5.1. PETROGRAPHIC DESCRIPTION

Rocks from the Syrian volcanism can be divided according to the figure 8 classification and a short review of the principal petrographic characters of the major rock types are given below.

Subalkaline basalts are holocrystalline with intersertal (± oriented) or subophitic texture. Microcrystalline texture is not common. The microphenocrists are generally olivine, sometimes plagioclase (An 50–60) or titan-augite. The plagioclase from the matrix is An 30–40. Titan-augite is

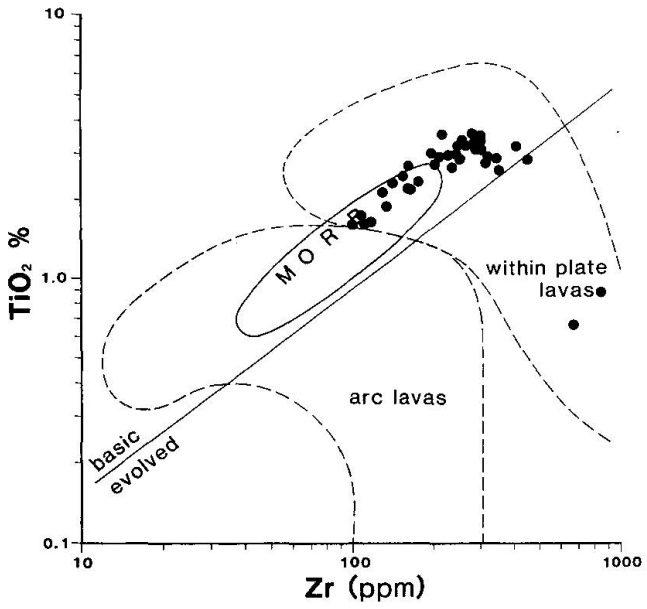

Fig. 9 Ti vs Zr diagram (PEARCE, 1980) showing the typical "Within Plate" character of all tertiary and quaternary basalts.

more common than diopsidic-augite. Opaque minerals and secondary calcite are abundant. Glass is infrequent. Iddingsite and chlorite represent the alteration minerals.

Alkaline basalts have intersertal, intergranular or microlithic textures. They can be oriented and are rarely amygdular. The microphenocrysts, sometimes megacrists, are olivine showing corrosion pattern, zoned titan-augite and plagioclase An 70–75. The plagioclase from the matrix is An 25–30. Some glass is present. Secondary minerals are iddingsite, sericite, chlorite, zeolites and calcite.

Hawaïtes have normally a fine-grained trachytic, occasionally an intergranular or microlithic texture. Plagioclase (An 35–65) microphenocrysts are often reabsorbed. In some samples, zoned and corroded titan-augite is associated to the plagioclase. Olivine is uncommon and generally completely transformed to iddingsite. In the matrix the plagioclase is An 0 to 15. Opaque grains are abundant.

Tephrite-basanites are microporphyric and present often vacuoles. Intergranular, intersertal

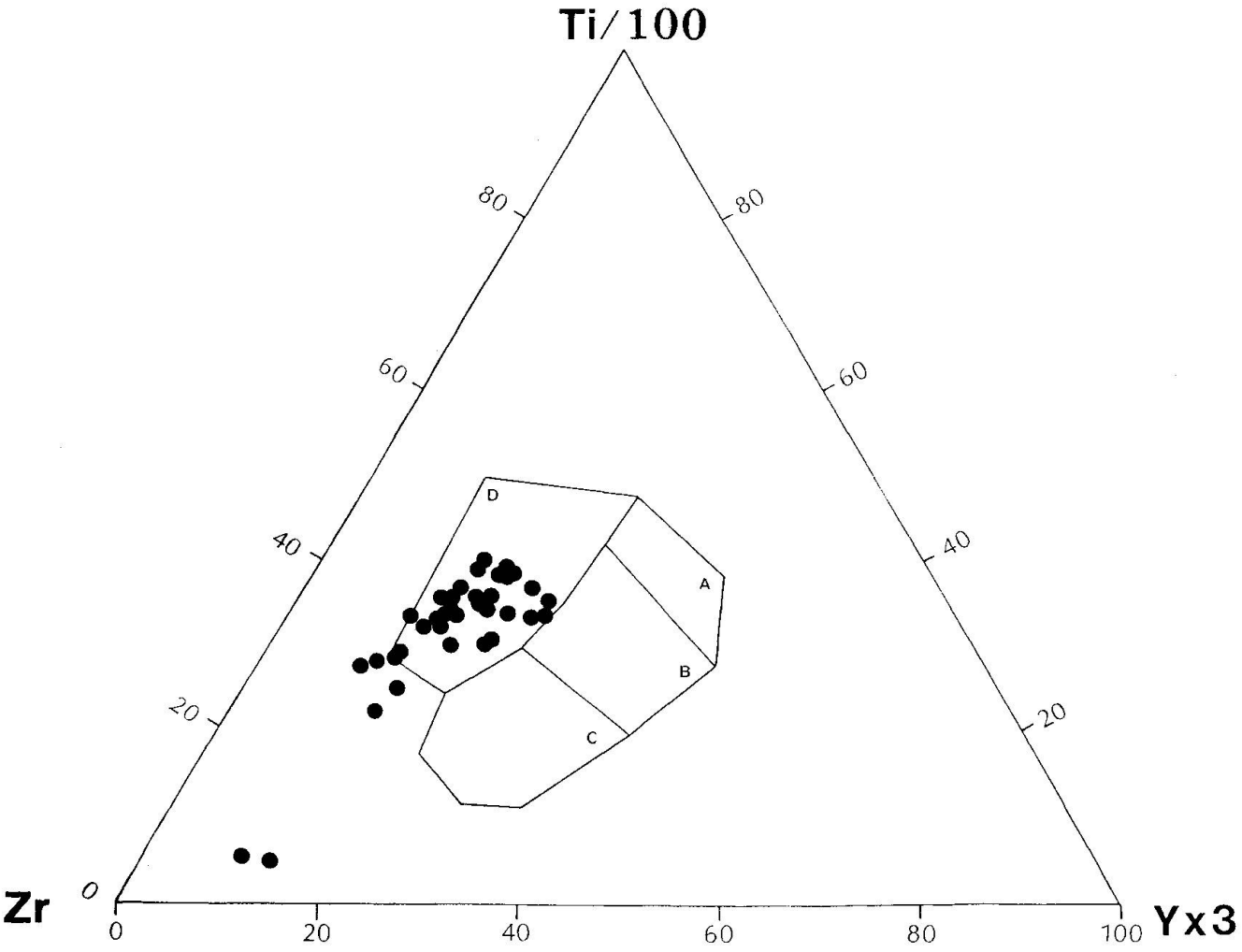

Fig. 10 Ti–Zr–Y differentiation diagram for Syrian basalts confirming also the "Within Plate" character.

of hyalopilitic textures are also seen. Glass in variable amount is more or less devitrified. Megacrysts are titan-augite and sometimes olivine. On the contrary, microphenocrysts are normally olivine and seldom augite. The plagioclase is An 35–55 in intersertal texture but An 0–5 in microlithic texture. Nepheline and opaque grains are present. Iddingsite, chlorite and calcite are the secondary minerals.

Trachytes. A single sample of trachyte has been found in the SW part of Syria. Its texture is trachytic microporphyric with microphenocrysts of sanidine in a matrix of alkaline plagioclase, amphibole, altered clinopyroxene and opaque minerals.

Xenoliths are common in most of the rocks described above. Wehrlites, anorthositic leucogabbros, noritic gabbros, grenatites and amphibolites have been recognized. Most of those originate from the upper mantle or from the deep continental crust and have been transported during the extrusion of the basaltic lavas.

5.2. CONCLUSIONS

The normative classification of the analysed rocks shows a distribution of the majority of points between the alkaline (nepheline normative) and the transitional zones (hypersthene normative). Only few of them are quartz normative tholeiites. No particular distribution of the various rock types can be related either to their geographical location nor to their age.

6. Conclusion

The intraplate basaltic volcanism along the Dead Sea Rift in Syria and Turkey was already active during Jurassic times but is not well represented and difficult to date precisely. During Cretaceous times, the activity is very well documented from Berriasian to Valanginian. Tertiary lavas show a gap between 16 and 8 Ma ago. This corresponds to the interval between both stages of spreading of the Red Sea – Dead Sea Rift system (CAMP and ROOBOL, 1989).

It is also clearly observed on the field that Jurassic and Cretaceous basalts erupted over very shallow water sediments or even on surfaces close to the sea level. During Palaeogene and Early Miocene, the basaltic flows where deposited on deep water sediments. Field evidences of the subsidence are numerous. Late Miocene, Pliocene and Pleistocene basalts are characteristic of subaerial volcanism.

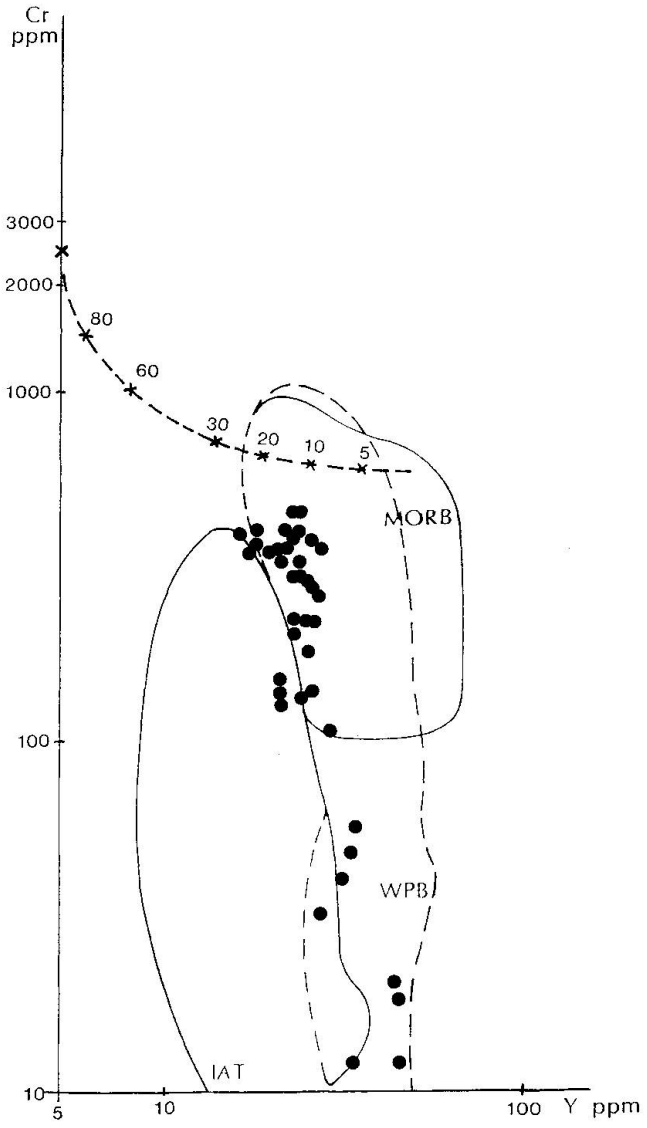

Fig. 11 Cr–Y differentiation diagram (PEARCE, 1980) indicating between 10 and 15% partial melting. This value is to be compared with that of figure 12.

FREUND et al. (1970) calculated a 105 km left-lateral mouvement along the Dead Sea Rift System in the area of the Red Sea. QUENNELL (1983) distinguished two phases: namely 62 km between Oligocene and Early Miocene and 45 km between Pliocene and Actual. This tectonic field observation is in good agreement with our potassium-argon dating further to the north. The 16–8 Ma gap is a major feature of the entire Rift.

In the central part of the Rift, the large folds of Mount Hermon and of the Palmyrides are the traces of a large amount of left-lateral mouvement.

In the Northern segment, the Rift is marked in Lebanon by the Yammimeh left slip fault (GAR-

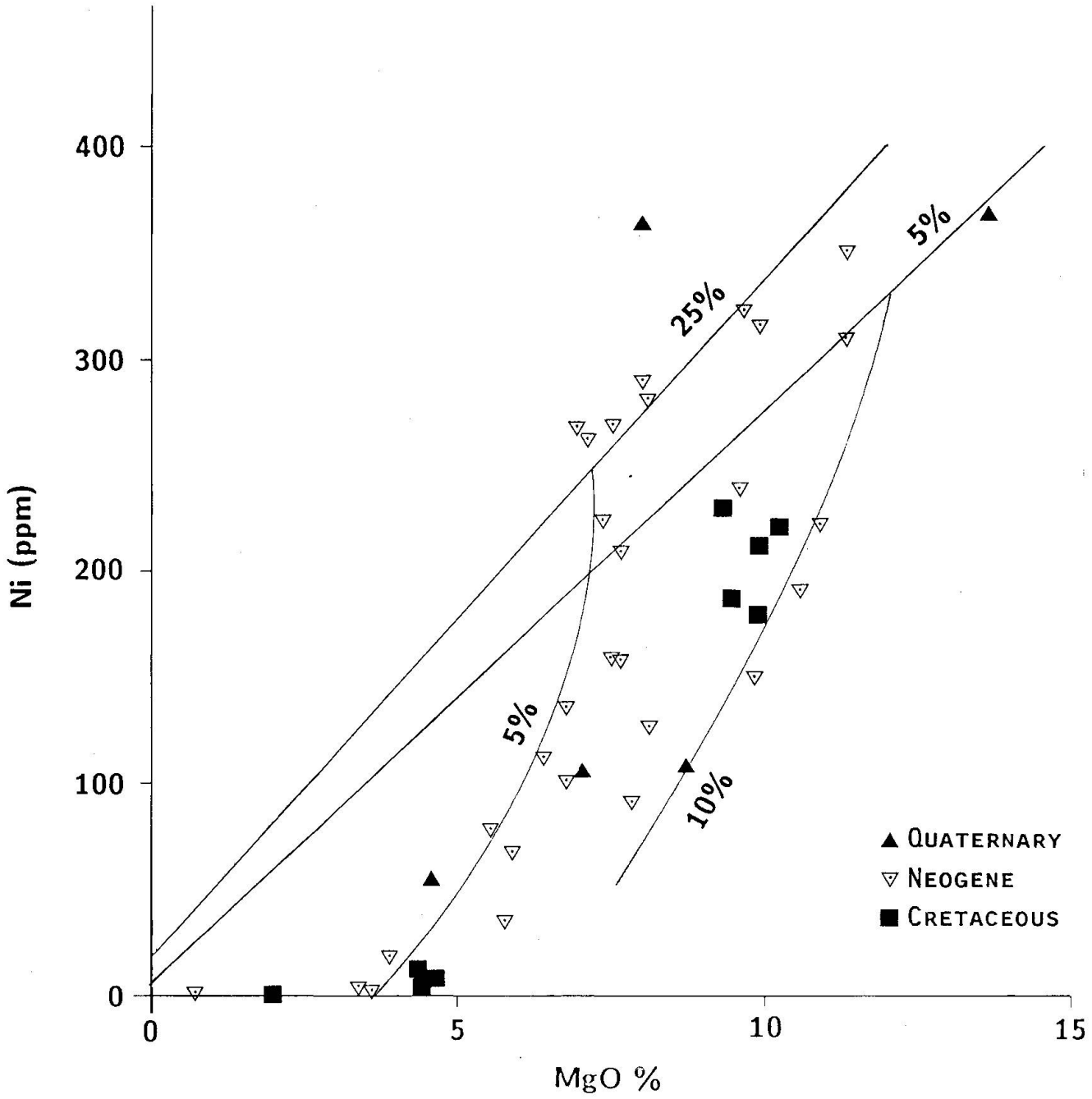

Fig. 12 Ni(ppm) vs MgO(%) diagram indicating the amount of partial melting and fractional crystallization (after AUCHAPT et al., 1987).

FUNKEL, 1981). It is flanked by mountains uplifted during Neogene times or later. Deep valleys (i.e. Rahb or Amik) oriented S–N are the traces of the Rift. Its northernmost portion is disturbed as it hits the Alpine Orogenic Belt of the Taurus and disappears at the junction with the Border Faults of the Croissant Peri Arab near Karaman-Maras in Turkey. The tholeitic plateau-basalt volcanism is also well represented in Afar (BARBERI et al., 1972; PILGER and RÖSSLER, 1976; COLEMAN and MCGUIRE, 1988) during the period of 36 to 15 Ma. According to these authors, it is the trace of crustal extension along the axis, better developped in Afar than in the Dead Sea Rift where the Arabian Plate only moved S–N without much of a rotation able to induce extension as well.

Acknowledgements

Field assistance by the Syrian Atomic Energy Commission supported the sample collection and survey. Finan-

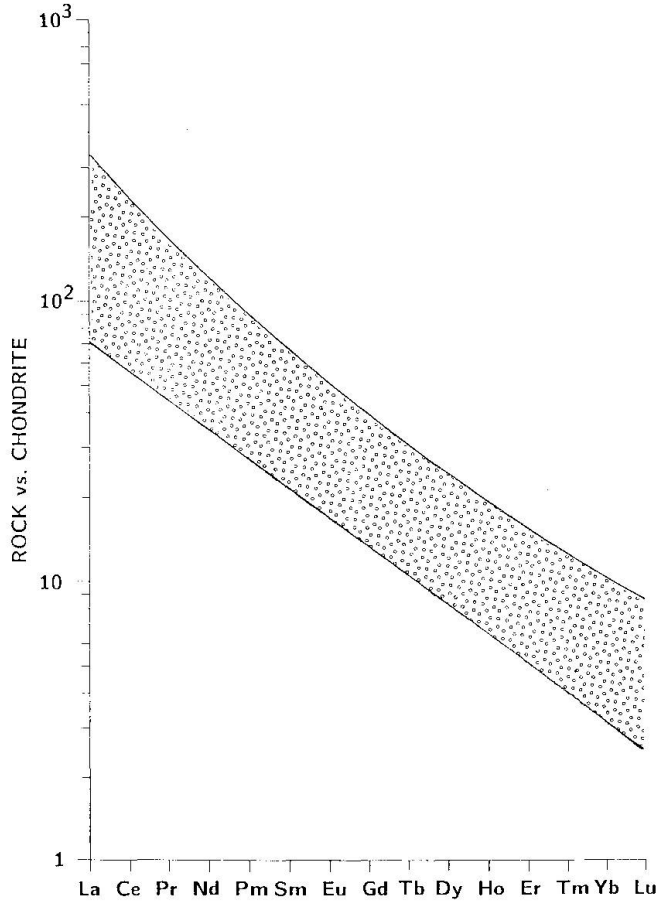

Fig. 13 Envelope of six REE pattern measured on whole rock samples.

cial support from the Swiss Research Foundation (grants 2.401.87 and 2.26551.89) is kindly acknowledged. Dr. P. Voldet measured the REE concentrations. Thanks are due also to Mrs Michèle Senn for her help with chemical analysis and CAD figures and to Mrs Marie-France Ingelsrud for argon measurements.

References

AUCHAPT, A., DUPUY, C., DOSTAL, J. and KAMIKA, M. (1987): Geochemistry and petrogenesis of Rift-related volcanic rocks from South Kivu (Zaire). J. Volc. Geotherm. Res., 31, 33–46.

BARBERI, F., BORSI, S., FERRARA, G., MARINELLI, G., SANTACROCE, R., TAZIEFF, H. and VARET, J. (1972): Evolution of the Danakil depression (Afar, Ethiopia) in light of radiometric age determinations. J. Geol. 80, 720–729.

BARBERI, F., CAPALDI, G., GASPERINI, P., MARINELLI, G., SANTACROCE, R., SCANDONE, R., TREUIL, M. and VARET, J. (1980): Recent basaltic volcanism in Jordan and its implication on the geodynamic history of the Dead Sea shear zone. In: Geodynamic evolution of the Afro-Arabian Rift System. Rep. Intern. Meeting, Rome 1979. Atti dei Convegni Lincei, 667–684.

CAMP, V.E. and ROOBOL, J.M. (1989): The Arabian continental alkali basalt province. Geol. Soc. Amer. Bull. 101, 71–95.

ÇAPAN, U.Z., VIDAL, PH. and CANTAGREL, J.M. (1987): K–Ar, Nd, Sr and Pb isotopic study of quaternary volcanism in Karasu valley (Hatay), N-end of Dead Sea Rift zone in SE-Turkey. Yerbilimleri, 14, 165–178.

DUBERTRET, L. (1933): Le Miocène en Syrie et au Liban. Notes et Mémoires Syrie et Liban, Vol. 1, 13–28.

DUBERTRET, L. (1937): Le Massif Alaouite. Notes et Mémoires Syrie et Liban, Vol. 2, 9–42.

DUBERTRET, L. (1940): Sur l'âge du volcanisme en Syrie et au Liban. C.R. Soc. Géol. France, 6, 55–57.

DUBERTRET, L. (1966): Liban, Syrie et bordure des pays voisins. Notes et Mémoires du Moyen-Orient, 8, 251–358.

DELALOYE, M. and WAGNER, J.-J. (1974): Potassium-Argon dating: an automatic equipment with digital output for computer processing. C.R. Soc. Phys. Hist. Nat. Genève, 9, 66–74.

FONTIGNIE, D. (1980): Géochronométrie K–Ar: Etude théorique et application à des matériaux des Flysch des Alpes occidentales. Thèse, Université de Genève.

FREUND, R., GARFUNKEL, Z., ZAK, I., GOLDBERG, M., WEISSBROD, T. and DERIN, B. (1970): The shear along the Dead Sea Rift. Philos. Trans. R. Soc. London, Ser. A, 267, 107–130.

HART, S.R. and DAVIS, K.E. (1978): Nickel partitioning between olivine and silicate melt. Earth Planet. Sc. Letters, 40, 203–219.

IRVINE, T.N. and BARAGAR, W.R.A. (1971): A guide to the chemical classification of common volcanic rocks. Can. J. Earth Sc., 8, 523–548.

MOUTY, M. and SAINT-MARC, P. (1982): Le Crétacé moyen du Massif Alaouite (NW de la Syrie). Cahiers de micropal., CNRS, Paris, 3, 55–69.

ODIN, G.S. (1982): Numerical dating in stratigraphy. John Wiley & Sons, Chichester, 2 vol., 1040 p.

PEARCE, J.A. (1980): Geochemical evidence for the genesis and eruptive setting of lavas from Tethyan ophiolites. In: Ophiolite, Proc. Intern. Symp. Cyprus, 1979, 261–272.

PEARCE, J.A. (1982): Trace elements characteristics of lavas from destructive plate boundaries. In: Andesites (R.S. Thorpe, ed.), 525–548.

PILGER, A. and RÖSSLER, A. (1976): Afar Depression of Ethiopia. Vol. 1. Schweizerbart, Stuttgart, 416 p.

PONIAKOV, V.P. (1966): The geological map of Syria, scale 1:1.000.000 and explanatory notes, 111 p.

QUENNELL, A.M. (1983): Evolution of the Dead Sea Rift – a review. In: A.M. Abed and H.M. Khled (eds), Geology of Jordan. Proc. 1st Jordanian Geol. Soc. Conf. Amman, 460–482.

QUENNELL, A.M. (1984): The western Arabia Rift System. In: The geological evolution of the Eastern Mediterranean (J.A. DIXON and A.H.F. ROBERTSON, eds). Geol. Soc. Special Publ., 17, 775–788.

VAUTRIN, H. (1934): Contribution à l'étude de la série jurassique dans la chaîne de l'Anti-Liban et plus particulièrement dans l'Hermon. C.R. Acad. Sc. Paris, 228, 198.

Manuscript received March 4, 1991; revised manuscript accepted November 1, 1991.